

Supplemental information

MDC1 maintains active elongation

complexes of RNA polymerase II

George Pappas, Sebastian Howen Nesgaard Munk, Kenji Watanabe, Quentin Thomas, Zita Gál, Helena Hagner Gram, MyungHee Lee, Daniel Gómez-Cabello, Dimitris Christos Kanellis, Pedro Olivares-Chauvet, Dorthe Helena Larsen, Lea Haarup Gregersen, Apolinar Maya-Mendoza, Panagiotis Galanos, and Jiri Bartek

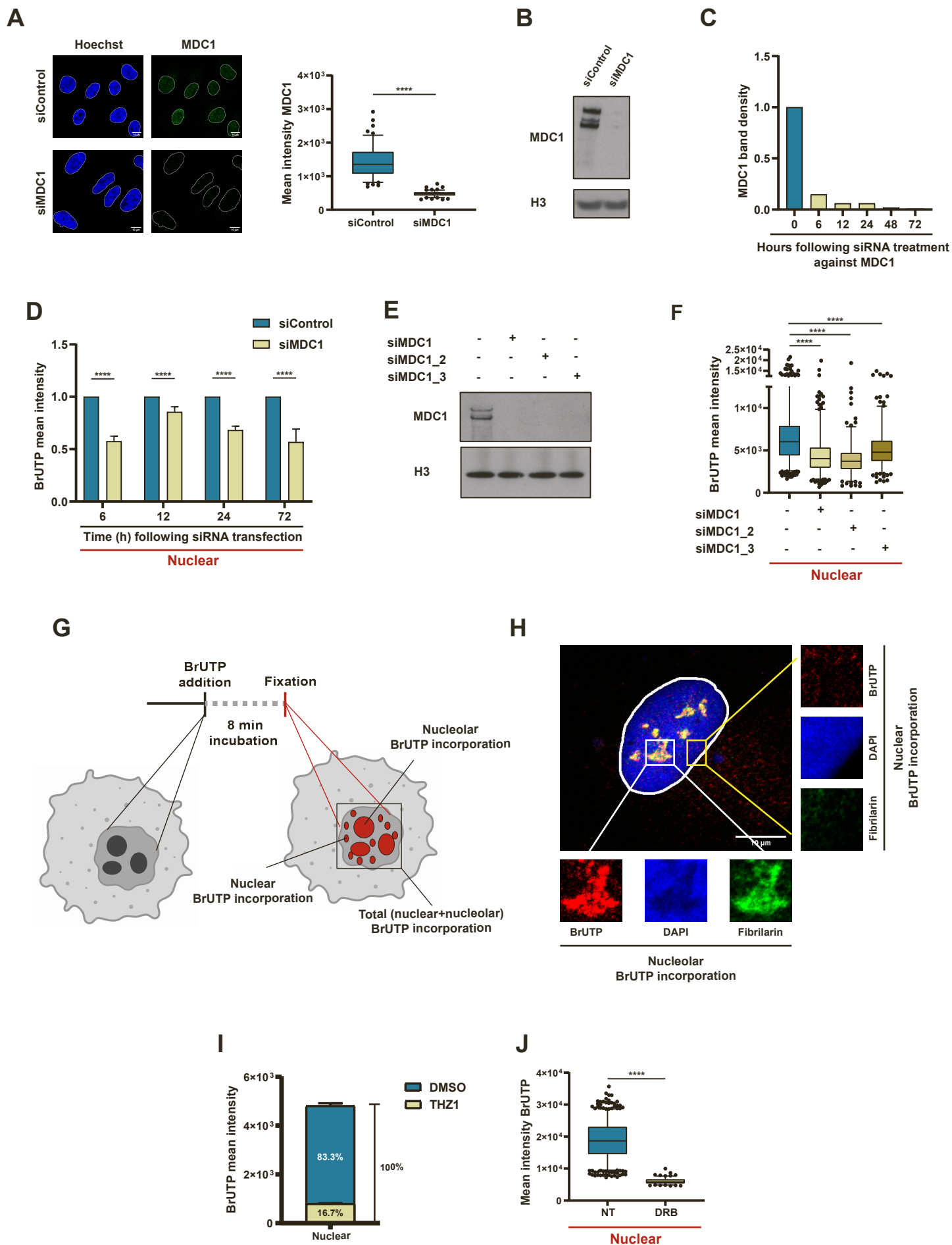


Figure S1. MDC1 facilitates RNA polymerase II activity. Related to figure 1.

(A) Representative images of U2OS cells immunostained for MDC1, upon transfection with the indicated siRNAs (Number of cells: $n > 100$). Individual values have been pooled together and data are represented as mean \pm SEM. Scale bar represents 10 μ m.

(B) Representative immunoblots of whole cell protein extracts (WCE) of U2OS cells transfected with the indicated siRNAs.

(C) Semi-quantification of MDC1 protein abundance following siRNA transfection.

(D) Quantification of nascent RNA synthesis in U2OS cells following siMDC1 transfection for the indicated time points (Number of cells irradiated: $n > 150$). Individual values have been pooled together and data are represented as mean \pm SEM.

(E) Representative immunoblots of whole cell protein extracts (WCE) of U2OS cells transfected with the indicated siRNAs.

(F) Quantification of nascent RNA synthesis in U2OS cells following transfection with the indicated siRNAs (Number of cells: $n > 150$). Individual values have been pooled together and data are represented as mean \pm SEM.

(G and H) BrUTP incorporation assay: Schematic representation and representative image of nuclear and nucleolar BrUTP incorporation. Scale bar represents 10 μ m.

(I) Quantification of nuclear nascent RNA synthesis upon treatment with THZ1 inhibitor (1 μ M for 1 hour) (Number of cells: $n > 100$). Individual values have been pooled together and data are represented as mean \pm SEM.

(J) Quantification of nuclear nascent RNA synthesis upon treatment with DRB inhibitor (100 μ M for 3.5 hours) (Number of cells: $n > 100$). Individual values have been pooled together and data are represented as mean \pm SEM.

**** $p < 0.0001$, by unpaired student t-test.

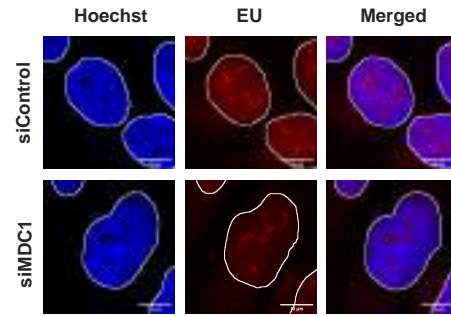
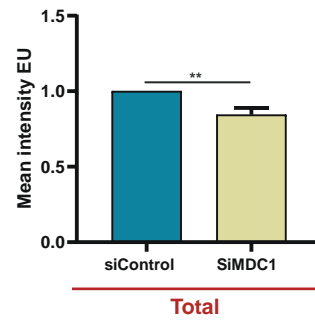
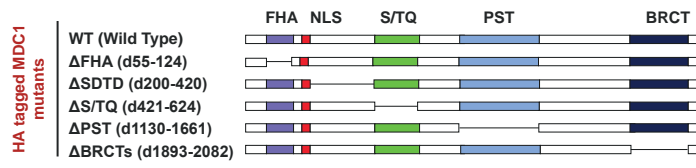
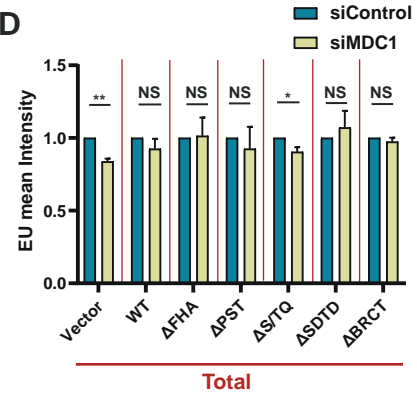
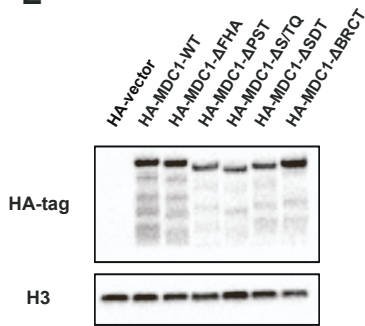
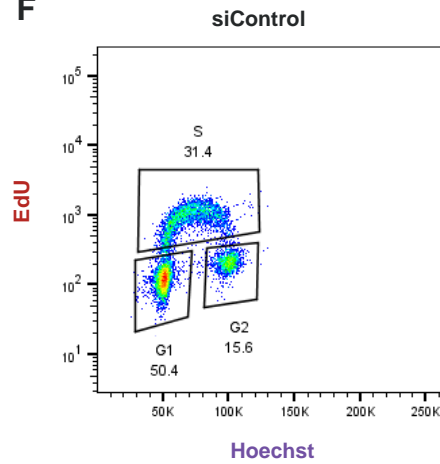
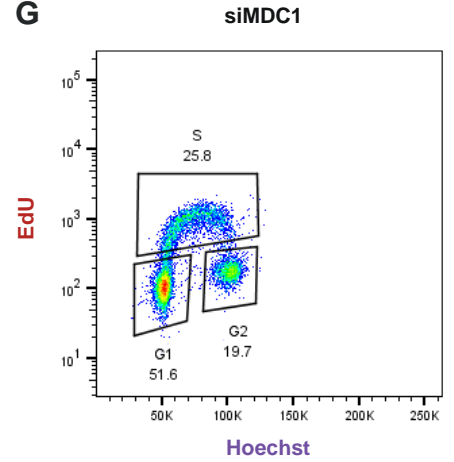
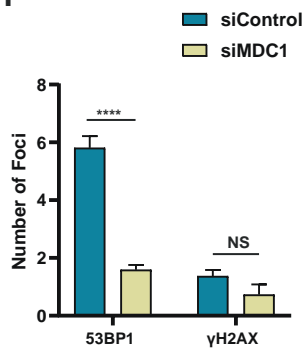
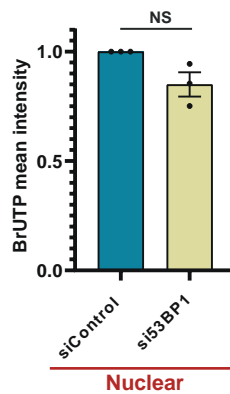
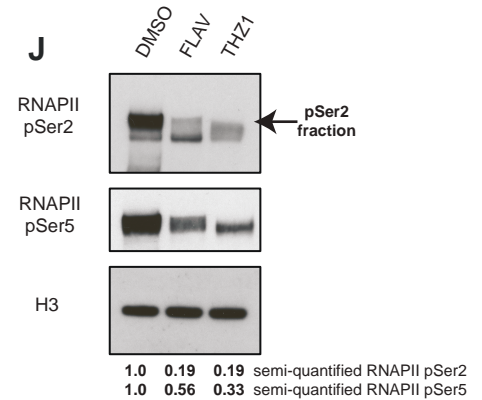
A**B****C****D****E****F****G****H****I****J**

Figure S2. MDC1 facilitates RNA polymerase II activity via its S/TQ domain without affecting genome integrity and cell cycle progression. Related to figure 1.

(A) Representative images of EU incorporation in U2OS, upon transfection with the indicated siRNAs. Scale bar represents 10µm.

(B) Relative quantification of EU incorporation in the whole nucleus of U2OS cells transfected with the indicated siRNAs using QIBC (Number of biological replicates: n=3). Biological replicates have been pooled together and data are represented as mean ± SEM.

(C) Schematic representation of HA-MDC1 deletion mutant plasmids.

(D) Relative quantification of whole nuclear EU incorporation upon transient overexpression of HA-MDC1 mutant constructs in U2OS cells transfected with the indicated siRNAs via QIBC. (Number of biological replicates: n=3. In each biological replicate the numbers of HA-positive cells varied from 50- 80 cells). Biological replicates have been pooled together and data are represented as mean ± SEM.

(E) Representative immunoblots of U2OS cells transfected with the indicated siRNA-resistant HA-MDC1 WT and mutant plasmids. Whole-cell protein extracts (WCE) were analyzed.

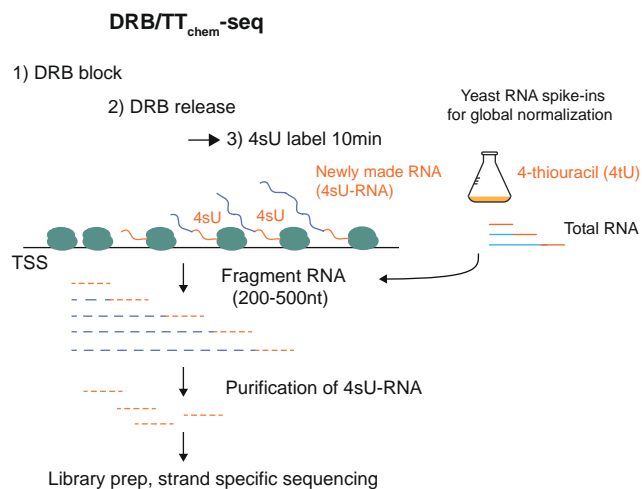
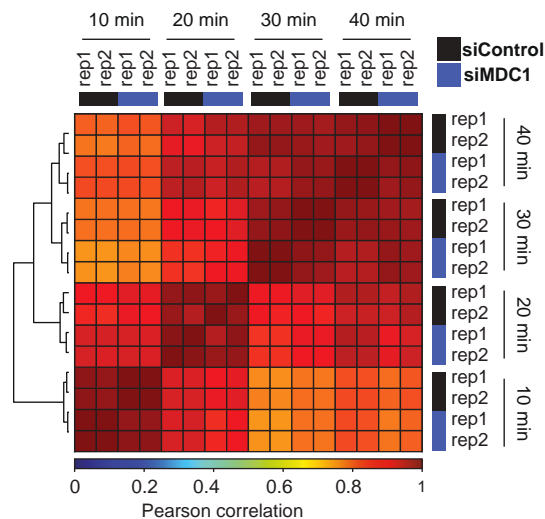
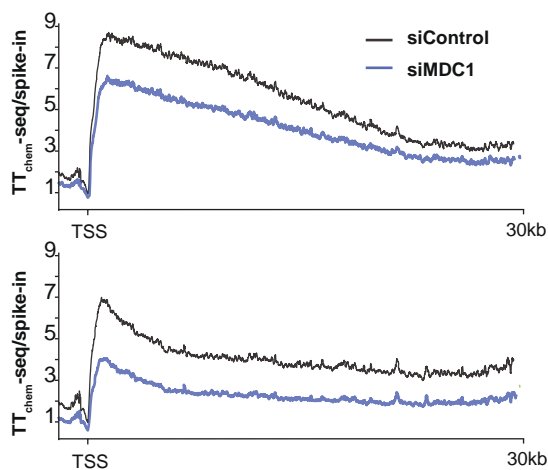
(F and G) Cell cycle profile of U2OS cells upon transfection with the indicated siRNAs.

(H) Analysis of DNA damage in U2OS cells upon transfection with the indicated siRNAs. Cells were pre-extracted and the number of 53BP1 and γH2AX foci was quantified via QIBC (Number of cells: n>3000). Individual values have been pooled together and data are represented as mean ± SEM.

(I) Relative quantification of nuclear nascent RNA synthesis in U2OS cells following si53BP1 transfection (Number of cells: n>150). Individual values have been pooled together and data are represented as mean ± SEM.

(J) Representative immunoblots of whole protein extracts and chromatin enriched fraction of the indicative proteins. Relative semi-quantification of band densities was carried out via Fiji (Image J). Arrow indicates pSer2 fraction.

NS, not significant; *p<0.05; **p<0.01; ****p<0.0001, by unpaired student t-test.

A**B****C****Short genes < 30kb (n=2329)****D****Medium length genes**

> 30kb and < 90kb (n=2379)

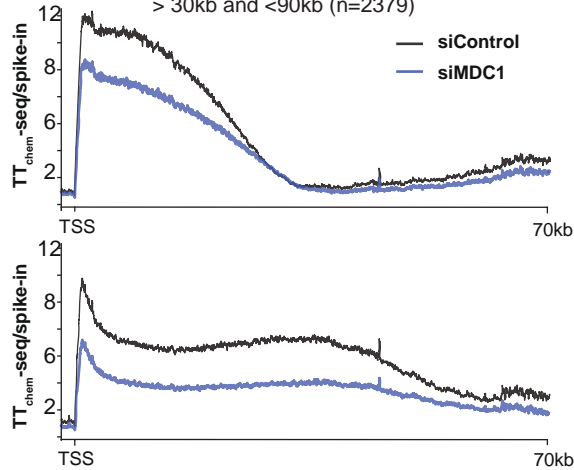
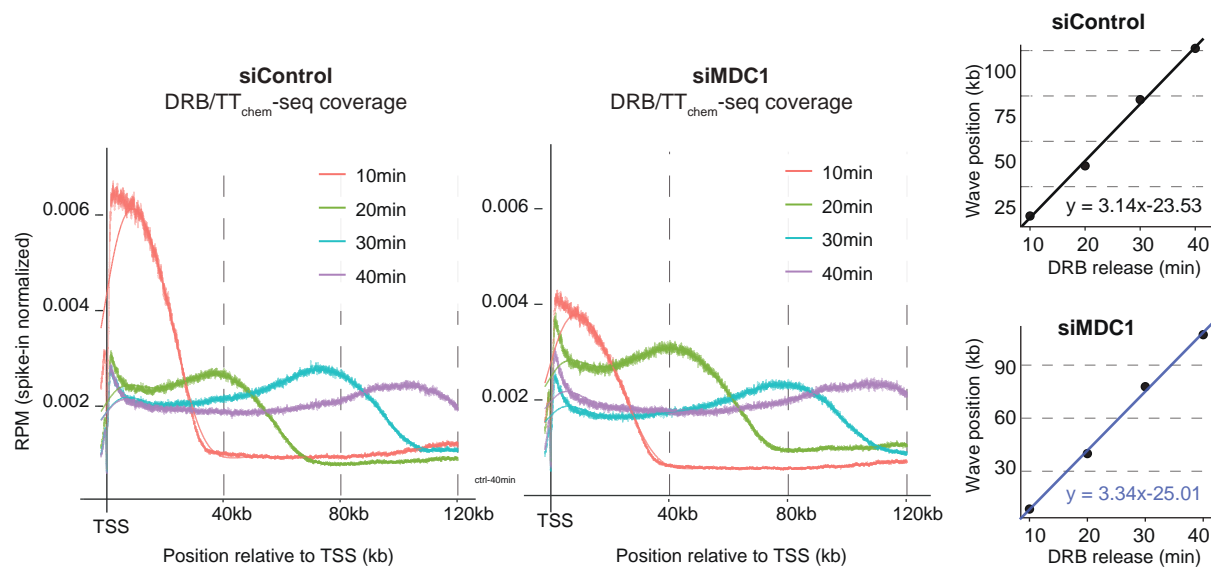
**E**

Figure S3: MDC1 impacts the engagement of RNAPII elongation complexes. Related to figure 3.

(A) Detailed overview of the workflow for DRB/TT_{chem}-seq, including generation of yeast spike-in normalization controls. Early elongation is blocked by the CDK9 inhibitor DRB, which leads to synchronization of all RNAPII complexes close to the TSS. After washing out of DRB, RNAPII complexes start elongating into the gene body and the progression can be tracked by TT_{chem}-seq. Here, nascent RNA is labeled *in vivo* by the addition of 4sU directly to the tissue culture medium. The reaction is stopped by TRIzol, and total RNA is extracted, spiked in with yeast RNA (4tU labelled), and fragmented by controlled base hydrolysis. 4sU residues in the fragmented RNA are biotinylated and used for streptavidin pull-down of 4sU-containing RNA.

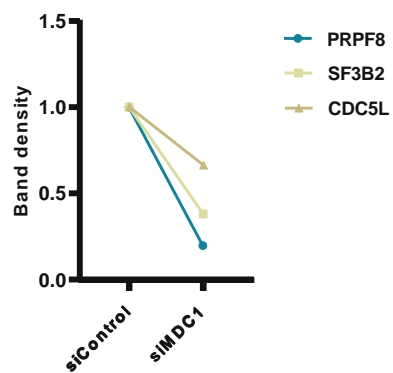
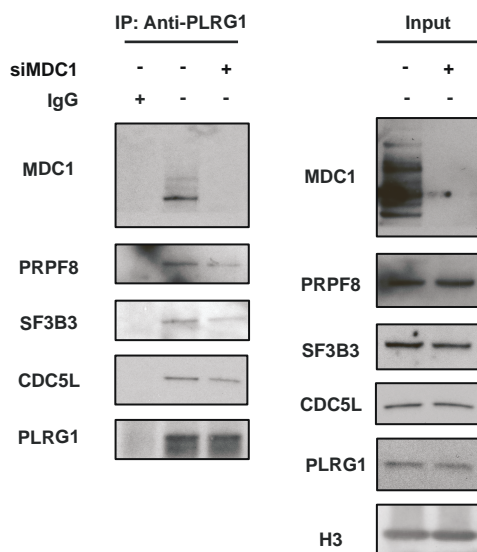
(B) Pearson's correlation matrix between each sample (siControl in black and siMDC1 in blue) and replicates calculated based on coverage from all protein-coding genes.

(C) Metagene profile of the average coverage normalized over spike-in and anchored at the TSS of non-overlapping protein-encoding genes with size below 30 kb ($n = 2,329$).

(D) Metagene profile of normalized over spike-in average coverage anchored at the TSS for non-overlapping protein-encoding genes with size above 30 kb and below 90 kb ($n = 2379$).

(E) DRB/TT_{chem}-seq metagene profiles for siControl (left) and siMDC1 (right) samples of protein-encoding genes between 80 and 300 kb from standard chromosomes (1–22,X,Y) with non-overlapping transcriptional units. The gene ranges were extended around their TSSs (–2 kb to +120 kb); any extensions beyond the limit of the chromosome were dropped ($n = 3,942$). lines are computationally fitted splines. Calculation of RNAPII elongation rates and linear regression equation for siControl and siMDC1 based on metagene profile.

A



B

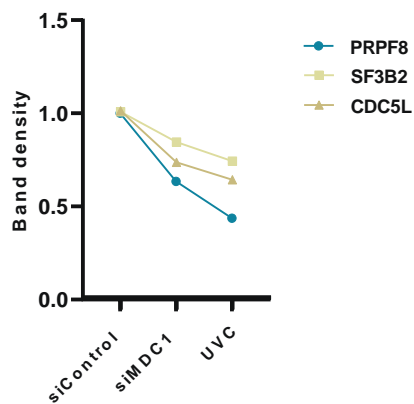
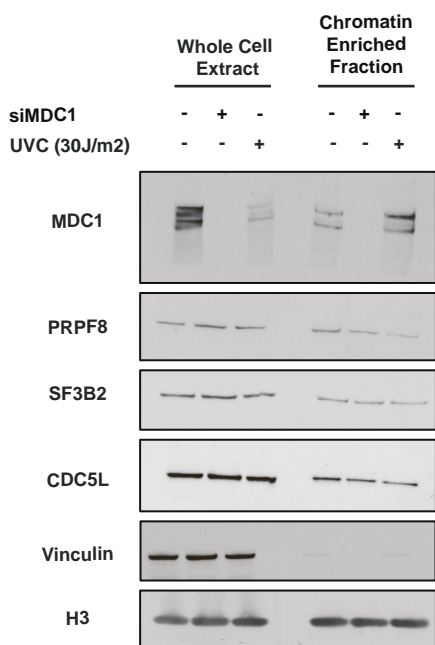


Figure S4: MDC1 knockdown impacts spliceosome assembly. Related to figure 4.

(A) Representative immunoblots of co-immunoprecipitation assay carried out by antibody against PLRG1 indicating its protein-protein interaction with different proteins of the spliceosome. Band densities were semi-quantified and plotted.

(B) Representative immunoblots of whole protein extracts and chromatin enriched fraction of the indicative proteins upon MDC1 knockdown and UVC irradiation. Band densities were semi-quantified and plotted.

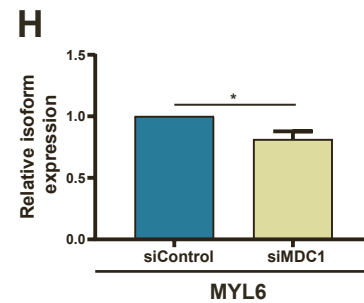
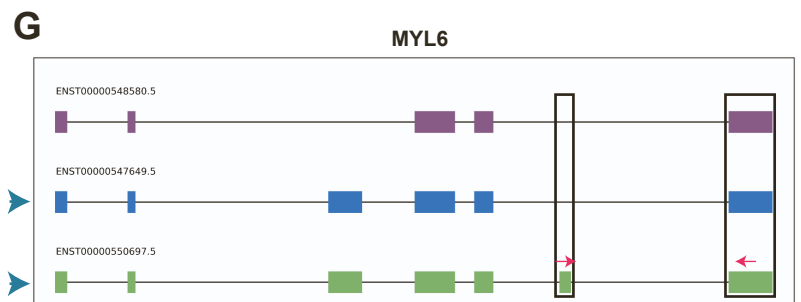
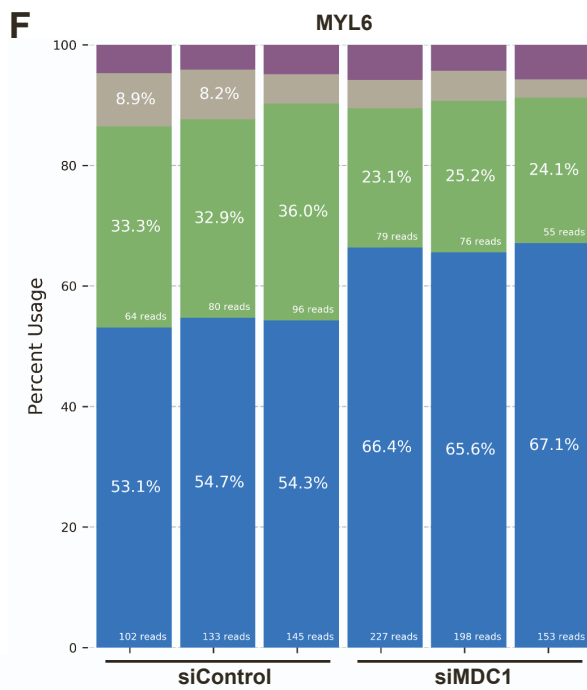
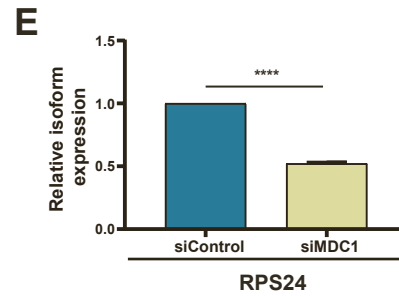
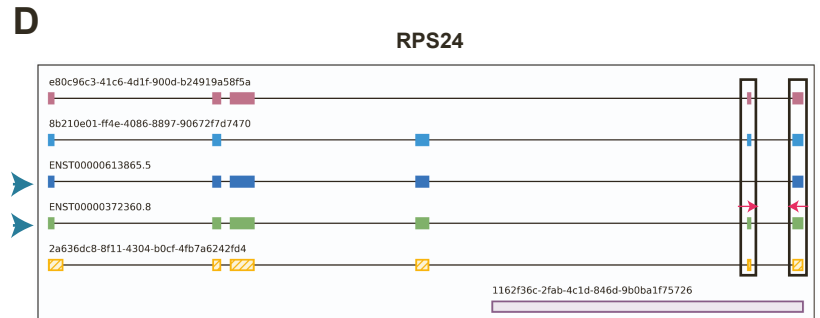
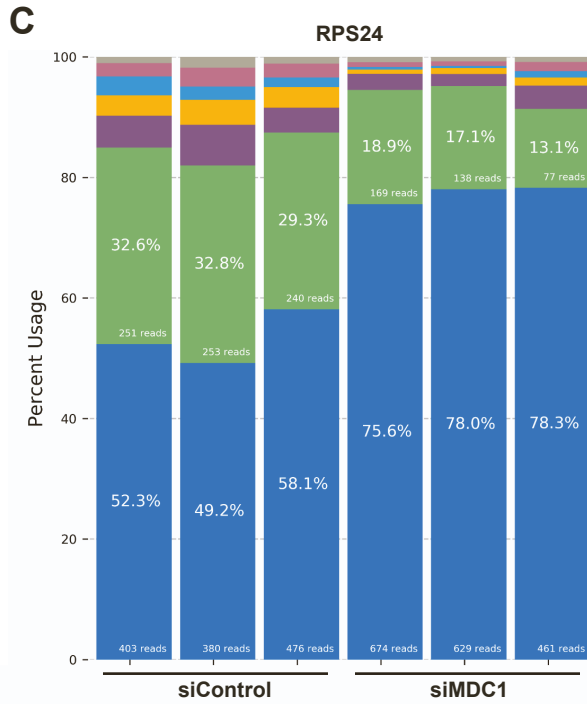
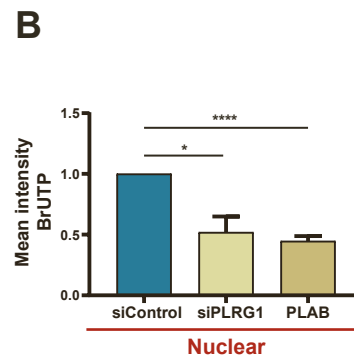
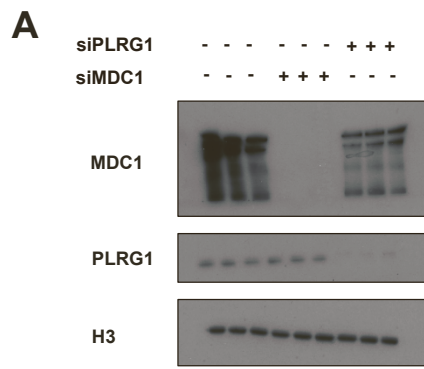


Figure S5: MDC1 induces changes in pre-mRNA splicing. Related to figure 5.

(A) U2OS cells were transfected with the indicated siRNAs and whole cell protein extracts (WCE) were immunoblotted with the indicated antibodies.

(B) Relative quantification of nuclear nascent RNA synthesis in U2OS cells following siPLRG1 transfection and treatment with PLAB inhibitor (Number of biological replicates: n=3 biological replicates). Biological replicates have been pooled together and data are represented as mean \pm SEM.

(C and D) Isoform usage changes in *RPS24*: Usage of the different isoforms detected in nanopore data with bar plot colors matching the corresponding isoforms. The two arrowheads indicate the two most abundant isoforms. The black brackets show the exon regions amplified with qPCR and the two red arrows indicate the primers designed for this purpose used in S5E (listed in table S1).

(E) qPCR was carried out using primers hybridizing to the chosen exon regions (Number of biological replicates: n=3 biological replicates). Biological replicates have been pooled together and data are represented as mean \pm SEM.

(F and G) Isoform usage changes in *MYL6*: Usage of the different isoforms detected in nanopore data with bar plot colors matching the corresponding isoforms. The two arrowheads indicate the two most abundant isoforms. The black brackets show the exon regions amplified with qPCR and the two red arrows indicate the primers designed for this purpose used in S5H (listed in table S1).

(H) qPCR was carried out using primers hybridizing to the chosen exon regions (Number of biological replicates: n=3 biological replicates). Biological replicates have been pooled together and data are represented as mean \pm SEM.

*p<0.05; ****p<0.0001, by unpaired student t-test.

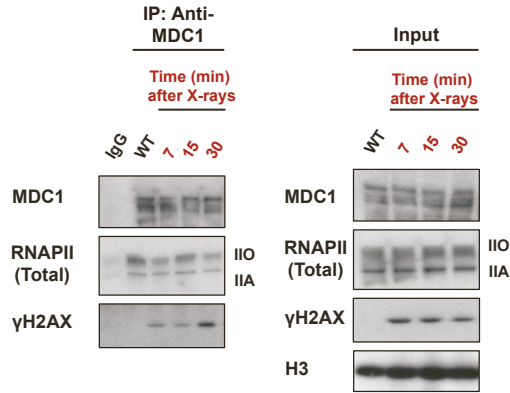
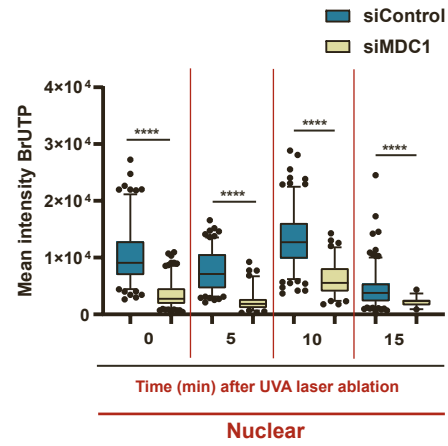
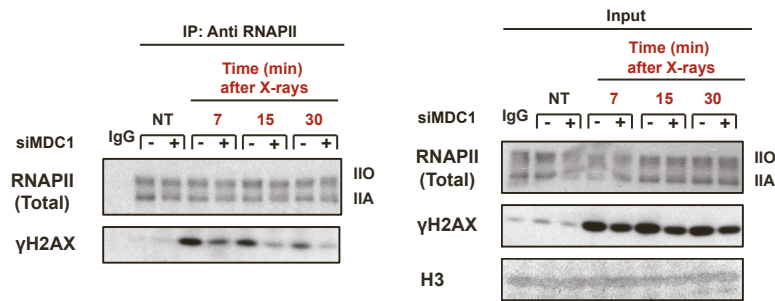
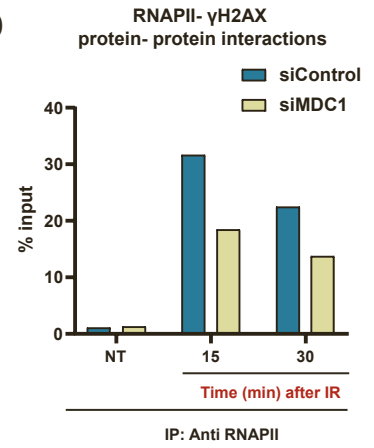
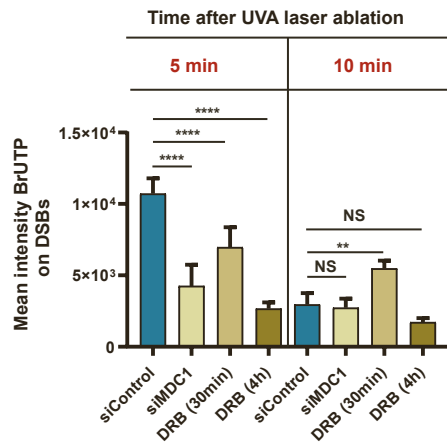
A**B****C****D****E**

Figure S6: MDC1 is required for RNAPII-mediated transcription on DSBs. Related to figures 6 and 7.

(A) Representative immunoblots of protein-protein interaction of MDC1, RNAPII and γ H2AX (IIO= phosphorylated RNAPII, IIA= non-phosphorylated RNAPII).

(B) Quantification of nuclear nascent RNA synthesis in U2OS cells following UVA laser ablation (Number of cells irradiated: $n > 20$). Individual values have been pooled together and data are represented as mean \pm SEM.

(C) Representative immunoblots showing protein-protein interactions between RNAPII and γ H2AX following X-rays upon transfection with the indicated siRNAs (IIO= phosphorylated RNAPII, IIA= non-phosphorylated RNAPII).

(D) Relative semi-quantification of protein-protein interactions between RNAPII and γ H2AX shown in S6C.

(E) Quantification of nascent RNA synthesis on DSB sites based on BrUTP incorporation. U2OS cells were transfected with the indicated siRNAs or incubated with DRB (100 μ M) for specific periods of time. (Number of irradiated cells: $n > 20$). Individual values have been pooled together and data are represented as mean \pm SEM.

NS, not significant; ** $p < 0.01$; **** $p < 0.0001$, by unpaired student t-test.

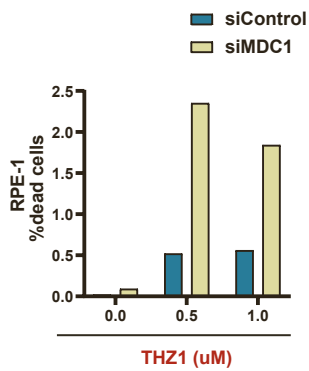
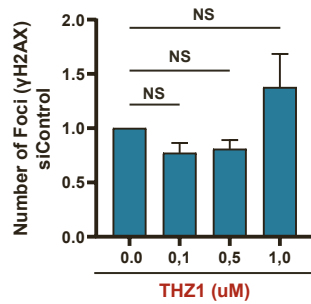
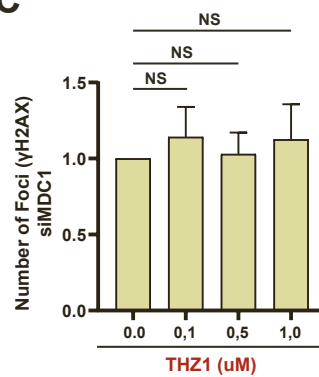
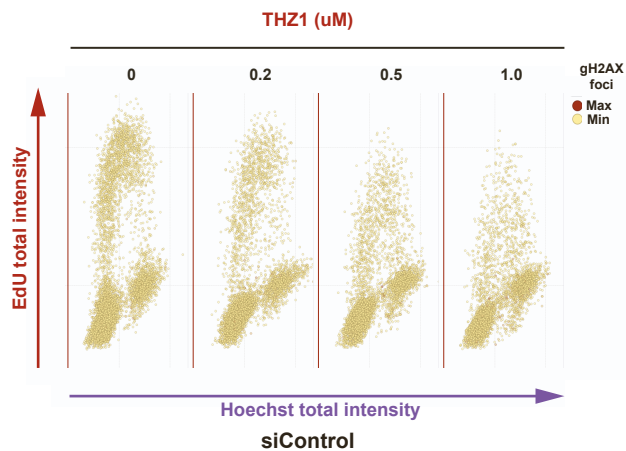
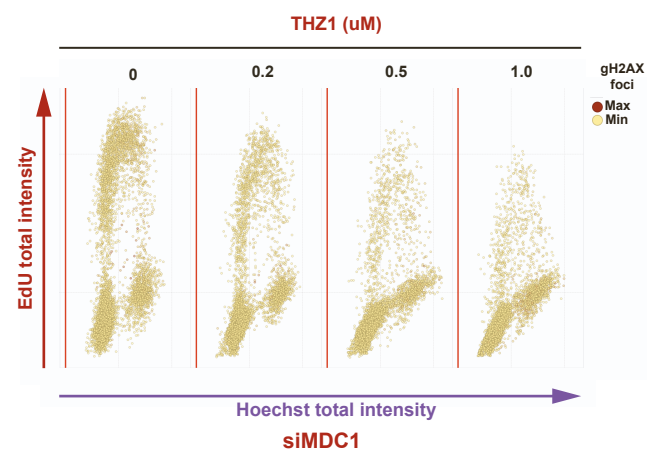
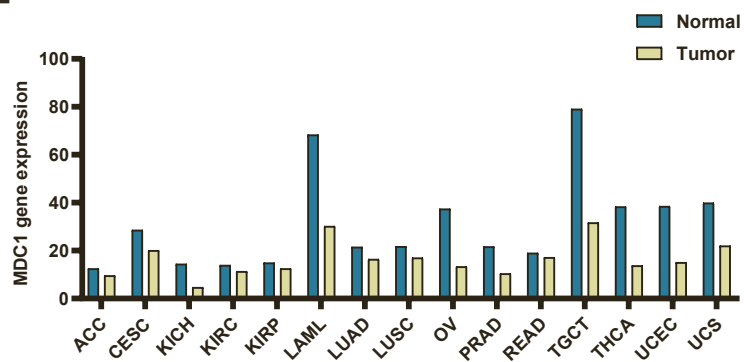
A**B****C****D****E****F**

Figure S7: MDC1 depletion sensitizes cells to THZ1. Related to figure 7.

(A) Representative bar plots of % dead cells of RPE-1 cells transfected with the indicated siRNAs upon THZ1 treatment (Experiment has been performed two times).

(B and C) Analysis of DNA damage in U2OS cells upon transfection with the indicated siRNAs followed by treatment with THZ1 inhibitor (48 hours of treatment) based on the quantification of γ H2AX foci via QIBC (Number of biological replicates: n= 3). Individual values have been pooled together and data are represented as mean \pm SEM.

(D and E) Cell cycle profile of U2OS cells transfected with the indicated siRNAs followed by treatment with THZ1 inhibitor (48 hours of treatment). The number of γ H2AX foci was analyzed in each cell cycle phase via QIBC.

(F) MDC1 gene expression levels in several cancer types. Data were acquired from Gepia database.

NS, not significant; by unpaired student t-test.

Table S1. DNA oligos and DNA primers. Related to figures 2, S2, and S5

qPCR Primers		
<i>MYL6</i> Forward: 5-GGCATGAGGACAGCAATGGT-3	This paper	N/A
<i>MYL6</i> Reverse: 5-CCCGACAGGATATGCCTCA-3	This paper	N/A
<i>RPS24</i> Forward: 5-GCAACGAAAGGAACGCAAGA-3	This paper	N/A
<i>RPS24</i> Reverse: 5-TGTGATCCAATCTCCAGCTCA-3	This paper	N/A
<i>GAPDH</i> Forward: 5-GAAACTGTGGCGTGATGGC-3	Singh J and Padgett R.A., 2009 [S1]	https://pubmed.ncbi.nlm.nih.gov/19820712/
<i>GAPDH</i> Reverse: 5-CACCACTGACACGTTGGCAG-3	Singh J and Padgett R.A., 2009 [S1]	https://pubmed.ncbi.nlm.nih.gov/19820712/
<i>ITPR1</i> Ex1 Forward: 5-TCTTCGCGGACATGGGATTACC-3	Singh J and Padgett R.A., 2009 [S1]	https://pubmed.ncbi.nlm.nih.gov/19820712/
<i>ITPR1</i> In1 Reverse: 5-GCATGCACATCCATCAAGATCTCCC-3	Singh J and Padgett R.A., 2009 [S1]	https://pubmed.ncbi.nlm.nih.gov/19820712/
<i>ITPR1</i> Ex5 Forward: 5-AGTTCTGGAAAGCCGCTAAGCC-3	Singh J and Padgett R.A., 2009 [S1]	https://pubmed.ncbi.nlm.nih.gov/19820712/
<i>ITPR1</i> In5 Reverse: 5-ACCAAGGCAGCCACTCACTACT-3	Singh J and Padgett R.A., 2009 [S1]	https://pubmed.ncbi.nlm.nih.gov/19820712/
<i>OPA1</i> Ex 18 Forward: 5-GGAACAGCTCTGAAAGCATTG-3	Singh J and Padgett R.A., 2009 [S1]	https://pubmed.ncbi.nlm.nih.gov/19820712/
<i>OPA1</i> Ex 19 Forward: 5-GGACAAGCATGCTAAAGGCACACC-3	Singh J and Padgett R.A., 2009 [S1]	https://pubmed.ncbi.nlm.nih.gov/19820712/
<i>OPA1</i> Ex 19 Reverse: 5-TCGTATGGATGCCAAAGATTGCCAG-3	Singh J and	https://pubmed.ncbi.nlm.nih.gov/19820712/

	Padgett R.A., 2009 [S1]	
MDC1 sequencing primers		
MDC1 seq primer #1: 5-CACCCAGGCTATTGACTGG-3	This Paper	N/A
MDC1 seq primer #2: 5-CTACTTCCTCCTCCGAGTCC-3	This Paper	N/A
MDC1 seq primer #3: 5-CTGATGCGGAAGAAGAGAGG-3	This Paper	N/A
MDC1 seq primer #4: 5-CCACACTGTCATCACTGTCC-3	This Paper	N/A
MDC1 seq primer #5: 5-AGAGAACAAACATGTGGGTGG-3	This Paper	N/A
MDC1 seq primer #6: 5-TCTGTCTCTGTTTCCCCTTGG-3	This Paper	N/A
MDC1 seq primer #7: 5-ATTGCAAGATGCCACCTGC-3	This Paper	N/A
MDC1 seq primer #8: 5-GGAAGGCTGGAGCTCAAGG-3	This Paper	N/A
MDC1 seq primer #9: 5-CTGAGCTCCAGATTTCCACC-3	This Paper	N/A
MDC1 seq primer #10: 5-CGGAAGCCTGTAGCTCAGG-3	This Paper	N/A
MDC1 seq primer #11: 5-CACAGACCAGTCCGTCACC-3	This Paper	N/A
MDC1 seq primer #12: 5-ACTGTCTTCTGGGAGACTTCC-3	This Paper	N/A
MDC1 seq primer #13: 5-TGAGATCTATGTGACCCCTGG-3	This Paper	N/A

Table S2. siRNAs against *MDC1* (siMDC1), *PLRG1* (siPLRG1), and Luciferase gene (siControl). Related to all figures 1-7 and S1-S7

siRNAs		
SiMDC1 sense: 5-UCCAGUGAAUCCUUGAGGU (dTdT)-3	Lou Z., et al., 2003 [S2]	https://pubmed.ncbi.nlm.nih.gov/12607004/
SiMDC1 anti-sense: 3-ACCUCAAGGAUUCACUGGA (dTdT)-5	Lou Z., et al., 2003 [S2]	https://pubmed.ncbi.nlm.nih.gov/12607004/
SiMDC1_2 sense: 5-GUUGUAAACUGAAAUCCAGC (dTdT)-3	Eliezer Y., et al., 2014 [S3]	https://pubmed.ncbi.nlm.nih.gov/24509855/
SiMDC1_2 anti-sense: 3-GCUGGAUUUCAGUUACAAC (dTdT)-5	Eliezer Y., et al., 2014 [S3]	https://pubmed.ncbi.nlm.nih.gov/24509855/
SiMDC1_3 sense: 5-AAUCCUGAGACCUCCUAAGGUUU (dTdT)-3	Goldberg M., et al., 2003 [S4]	https://pubmed.ncbi.nlm.nih.gov/12607003/
SiMDC1_3 anti-sense: 3-AAACCUUAGGAGGUCUCAGGAUU (dGdT)-5	Goldberg M., et al., 2003 [S4]	https://pubmed.ncbi.nlm.nih.gov/12607003/

SiPLRG1_1 sense: 5-UCAUAAACAGUACCCUGCCAAUCAA (dTdT)-3	Mu R., et al., 2014 [S5]	https://pubmed.ncbi.nlm.nih.gov/24675469/
SiPLRG1_1 anti-sense: 3-UUGAUUGGCAGGGUACUGUUUAUGA (dAdA)-5	Mu R., et al., 2014 [S5]	https://pubmed.ncbi.nlm.nih.gov/24675469/
SiPLRG1_2 sense: 5-CCACCGUGGAAACUCUACAGGGUUA (dTdT)-3	Eurofins Genomics	N/A
SiPLRG1_2 anti-sense: 3-UAACCCUGUGAGGUUCCACGGUGG (dTdG)-5	Eurofins Genomics	N/A
SiGL3 (Luciferase) sense: 5-CUUACGCUGAGUACUUCGA (dTdT)-3	Lubas M., et al., 2015 [S6]	https://pubmed.ncbi.nlm.nih.gov/25578728/
SiGL3 (Luciferase) anti-sense: 3-UCGAAGUACUCAGCGUAAG (dTdT)-5	Lubas M., et al., 2015 [S6]	https://pubmed.ncbi.nlm.nih.gov/25578728/

1. Singh, J., and Padgett, R.A. (2009). Rates of in situ transcription and splicing in large human genes. *Nature structural & molecular biology* 16, 1128-1133. 10.1038/nsmb.1666.
2. Lou, Z., Minter-Dykhouse, K., Wu, X., and Chen, J. (2003). MDC1 is coupled to activated CHK2 in mammalian DNA damage response pathways. *Nature* 421, 957-961. 10.1038/nature01447.
3. Eliezer, Y., Argaman, L., Kornowski, M., Roniger, M., and Goldberg, M. (2014). Interplay between the DNA damage proteins MDC1 and ATM in the regulation of the spindle assembly checkpoint. *The Journal of biological chemistry* 289, 8182-8193. 10.1074/jbc.M113.532739.
4. Goldberg, M., Stucki, M., Falck, J., D'Amours, D., Rahman, D., Pappin, D., Bartek, J., and Jackson, S.P. (2003). MDC1 is required for the intra-S-phase DNA damage checkpoint. *Nature* 421, 952-956. 10.1038/nature01445.
5. Mu, R., Wang, Y.B., Wu, M., Yang, Y., Song, W., Li, T., Zhang, W.N., Tan, B., Li, A.L., Wang, N., et al. (2014). Depletion of pre-mRNA splicing factor Cdc5L inhibits mitotic progression and triggers mitotic catastrophe. *Cell death & disease* 5, e1151. 10.1038/cddis.2014.117.
6. Lubas, M., Andersen, P.R., Schein, A., Dziembowski, A., Kudla, G., and Jensen, T.H. (2015). The human nuclear exosome targeting complex is loaded onto newly synthesized RNA to direct early ribonucleolysis. *Cell reports* 10, 178-192. 10.1016/j.celrep.2014.12.026.